On the Autonomous Inspection and Classification of Marine Growth on Subsea Structures

Liniger, Jesper; Jensen, Anna Lyhne; Pedersen, Simon; Sørensen, Henrik; Mai, Christian

Published in:
Proceedings of 2022 OCEANS Conference & Exposition, Oceans 2022 Chennai

DOI (link to publication from Publisher):
10.1109/OCEANSChennai45887.2022.9775295

Publication date:
2022

Document Version
Accepted author manuscript, peer reviewed version

On the Autonomous Inspection and Classification of Marine Growth on Subsea Structures

Jesper Liniger
AAU Energy
Aalborg University
Esbjerg, Denmark
jel@energy.aau.dk

Anna Lyhne Jensen
AAU Energy
Aalborg University
Aalborg, Denmark
alj@energy.aau.dk

Simon Pedersen
AAU Energy
Aalborg University
Esbjerg, Denmark
spe@energy.aau.dk

Henrik Sørensen
AAU Energy
Aalborg University
Aalborg, Denmark
hs@energy.aau.dk

Christian Mai
AAU Energy
Aalborg University
Esbjerg, Denmark
chrimai@energy.aau.dk

***Abstract*—Marine growth challenges the structural integrity of offshore facilities due to increased hydro dynamical loads. As a consequence, marine growth cleaning on offshore structures has been performed for many years. While the industry has shifted from diver-assisted to cleaning driven by remotely operated vehicles, the process remains costly and ineffective. This paper explores the possibilities for introducing an increased level of automation for marine growth inspection and classification. Specific attention is given to sensor technologies and methods for constructing a 3D representation of the offshore structures in order to assess the thickness and composition of marine growth. While optical-based methods show positive potential further work is needed to investigate the robustness to flicking sunlight and turbidity issues experienced in areas close to the water surface. The review of classification methods reveals several promising approaches where deep learning is applied for the categorization of marine growth. The training relies on large databases of relevant images which are not currently available for marine growth on offshore structures. Further work is needed for investigating if virtual images can be used in combination with a reduced set of real images.**

***Index Terms*—ROV, Marine Growth, 3D reconstruction, SfM, Stereo Vision, Structured Light, Time of Flight, Machine Learning, Classification**

I. Introduction

Marine growth (MG), also termed bio-fouling, is a phenomenon occurring for a hard-surfaced structure submerged in seawater. Over time, the surface of such structures will be populated by marine organisms. Affecting the weight, size, and surface of submersed structures, marine growth poses a significant issue for both the marine transportation sector and offshore structures in the energy sector. This work takes an offset in the latter, which is currently dominated by the Oil & Gas (O&G) production and offshore wind turbines.

Offshore O&G production facilities and shallow water wind turbines are predominantly installed on jacket-type structures. Such grid element structures are especially sensitive to marine growth due to a drastically enlarged surface area and roughness, which increases the hydrodynamic loads from waves and tidal streams [1]–[5]. The increase in hydrodynamic loads is a lifetime limiting factor and dependent on the thickness and composition of marine growth, often categorized as hard or soft. To accommodate the increase in these loads, the jacket structures are designed to handle marine growth up to a specified thickness and composition [6]. A marine growth removal campaign is issued if the specifications are exceeded.

The need for inspection and removal of marine growth is not expected to be affected by future decommissioning of O&G production facilities. In fact, an increase is expected with the introduction of deep water renewable energy facilities such as floating wind turbines and wave point absorbers which are both susceptible to issues caused by marine growth [7], [8].

II. Current State of Marine Growth Inspection

Historically, inspection has been facilitated by divers. Due to the safety of the personnel working close to the structures, the allowable weather conditions reduce the window of operation significantly, which causes high operational costs. Currently, the inspection process has almost entirely shifted to the use of Remotely Operated Vehicles (ROV) manually controlled by personnel located on a vessel. ROVs can be deployed in a wider range of weather conditions which reduces the duration of a cleaning campaign.

The current state of the cleaning process is seen in Fig. 1.

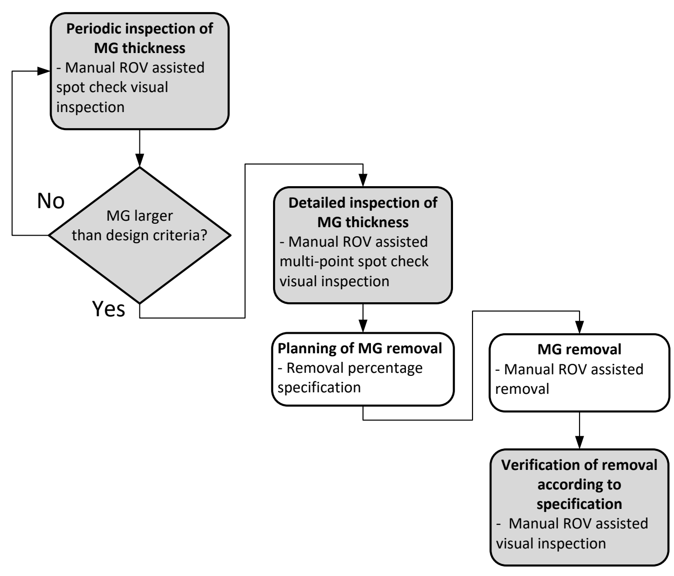

Fig. 1. Marine growth removal process. The grey boxes indicate the events investigated in this paper with a focus on the potential for automation.

The process is initialized by an inspection phase where an ROV is used for conducting spot checks on the structure. Figure 2 shows the method used during the initial inspection phase. Spot checks are made using a probe acting as a ruler mounted on the ROV which is pushed into the marine growth. The operator then evaluates the thickness, composition, and percentage cover of marine growth based on video feedback from the ROV. The composition of MG is considered due to the effective diameter difference for soft vs. hard MG as illustrated in Fig. 3. The forces from waves and tidal streams are proportional to the effective diameter. Therefore, a greater thickness of soft MG is allowed before cleaning is issued. Mussels, barnacles, and tube worms are examples of hard MG while sea squirts, seaweeds, and sea anemones are examples of soft MG. Since MG depends on sunlight and the thickness is usually larger near the water surface and reduces as light is attenuated. Usually the effect and thickness of MG is negligible below 30m. Typical examples of allowable MG thicknesses range from 0.1m for hard MG to 1m for soft MG. Other than the thickness and composition, also the percentage of the structure covered is used for planning the extent of cleaning.

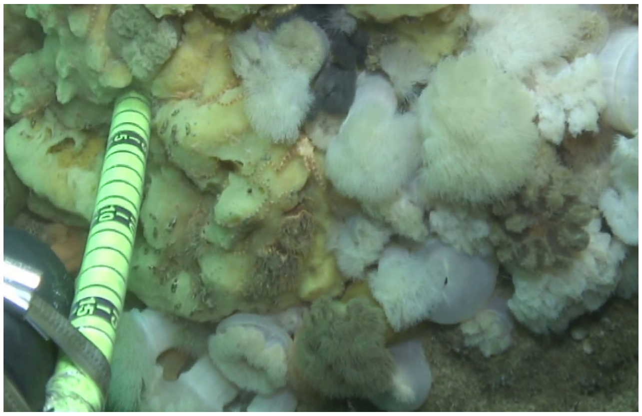

Fig. 2. Manual ROV assisted marine growth inspection [9]

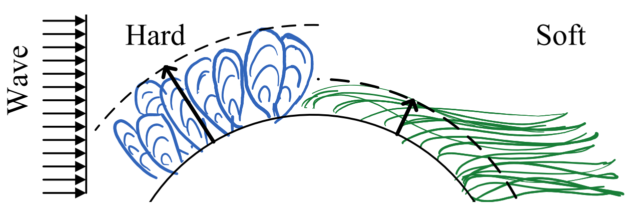

Fig. 3. Effective thickness illustration for hard and soft marine growth on a structural element.

A detailed inspection employing a more extensive grid of spot checks is issued if the MG specifications are exceeded. A cleaning campaign is then planned and performed to the affected areas of the structure. After cleaning, the amount of removed MG is verified. The verification is conducted by performing a manual evaluation of video feedback from spot checks on the structure.

Despite the use of ROVs, a cleaning campaign remains one of the most labor and cost-intensive maintenance operations of offshore structures. In addition, the precision obtained using only manual spot checks on the structure leads to significant uncertainties on both the initial MG inspection and final verification of removed MG.

This paper will explore the available methods for reducing both the operational costs and uncertainty of inspection results by means of automation. Firstly, the instrumentation technologies applicable for autonomous marine growth detection will be reviewed, followed by a review of methods on the classification of the marine growth composition. It is recognized that automation of the MG removal process itself will further reduce the cost of the cleaning campaign. The possibilities for automation of MG removal are investigated in the work by Pedersen et al. [10].

III. Sensor Technologies for Marine Growth Inspection

This section will explore the available sensor technologies and techniques needed for assessing MG on subsea structures. The range and field of view requirements are dependent on the diameter of the structural elements considered for inspection. In this study, we use the diameter of jacket-type, monopile, and floating foundations as given in Tab. I. It is noted that dimensions of monopile foundations for wind turbines are typically selected to withstand the increased forces from MG and, therefore, require no cleaning. Nevertheless, monopiles are considered since the trade-off between maintenance costs of cleaning and material costs can shift due to the advantages of automation of MG removal.

TABLE I
Subsea structural element diameters for different foundations types.

Foundation type	**Diameter range [m]**	**Reference**
Jacket (wind and O&G)	0.95 - 1.8	[11]
Monopile	3 - 9.5	[11], [12]
Floating	2.2 - 4.3	[13]

The review is divided into optical and acoustical sensor technologies. The reviewed technologies applicable for MG inspection are listed in Tab. II.

TABLE II
Sensor technologies applicable for MG inspection. Primarily based in reviews by Chimesky et al. [14], Menna et al. [15], Massot-Campos and Oliver-Codina [16], and Xi et al. [17]

Technology	**Range [m]**	**Cost**
Optical		
Structure from Motion (SfM)	<3	Low
Stereo Vision (SV)	<3	Low
Structured Light (SL)	<10	Medium
Laser Line Scanner (LLS)	<10	High
Time-of-Flight (ToF)	<10	Medium-High
Acoustical		
Multi Beam Sonar (MBS) ($>$1Mhz)	<10	High

A. Optical methods

Conceptually, the current spot-check method for MG thickness estimation relies on a manual inspection of optical feedback from a camera facing toward the probe. However, to reduce the uncertainty inflicted by spot-checking, the reviewed methods focus on recreating a 3D representation of the MG on the structure. Optical 3D reconstruction techniques are extensively researched and have found many applications on e.g. ground robots and Unmanned Areal Vehicles (UAVs) [18]. However, the in-air optical methods are not directly applicable in an underwater scenario. Non-homogeneous and irregular light attenuation in the water column, narrow transmission window (470-580nm), sediment-induced light scattering, and polarization are among the challenges faced for underwater optical methods [16], [19], [20].

With additions, the following description is based on the comprehensive reviews of optical methods for underwater applications conducted by Chemisky et al. [14], Menna et al. [15], Massot-Campos and Oliver-Codina [16], and Xi et al. [17].

1) Passive methods: Two of the typical *passive* optical reconstruction techniques are Structure from Motion (SFM) and Stereo Vision (SV), which both use images of the scene to reconstruct 3D information.

Structure from Motion (SfM) uses a series of images from a single camera source for reconstructing a 3D scene. The 3D scene is constructed from triangulation of detected identical features from a series of images [21]. A scaling problem arises for the constructed 3D scene since the distance from the observer to the features is unknown. This ambiguity can be resolved using calibration targets with known sizes, which can be either inherent in the scene (e.g. known structural elements) or ones added manually (e.g. tape measure, printed calibration targets). Several underwater experimental results (with calibrated targets) showed an accuracy of 10mm using the Scale Invariant Feature Transform (SIFT) [22], [23] and the highest accuracy of 0.7mm was obtained using the Speed Up Robust Features (SURF) [24]. While this accuracy is sufficient for MG thickness estimation, the range limitation below 3m and drift issues are the main challenges for using this method on larger diameter structures [14].

As marine growth classification often relies on color imagery, Bryson et al. showed that color information could be recreated on 3D models obtained from SfM by using full water attenuation color correction [25]. Liu et al. [26] reviewed technology for Underwater Hyperspectral Imaging (UHI), which in combination with color enhancement techniques provide an opportunity for improving subsequent MG classification based on SfM 3D scenes.

While SfM is easy to employ and yields a very cost-effective solution due to the simple equipment requirement (a monocular camera), the method is only viable at close range and needs rigid scenes with clear textures to achieve full coverage. Specifically, soft MG is non-rigid which imposes an issue when triangulation is performed. The method is also affected by poor visibility and flickering from sunlight when operating close to the surface, which is where structures are known to be most affected by MG [14], [16]. Further investigation is also needed to assess if the textures of MG are sufficient for SfM in a setting close to an offshore structure.

Stereo Vision (SV), a technique related to SFM, uses triangulation from detected features similarly to SfM but applies two cameras pointed toward a common scene. By utilizing the known distance and orientation of the cameras, the scaling problem of SfM is avoided. Apart from providing fixed scaling, and some redundancy in the images, SV is generally affected by the same problems known for SfM. A stereo vision technique has increased cost over SfM since a minimum of one extra camera is needed [14].

The passive methods both rely on robust feature detection, which can be difficult to reliably achieve in real-world subsea conditions; Reggiannini and Moroni [27] highlight, in a recent review, the advantage of using machine learning for feature detection to increase the performance of feature detection in low texture underwater environments.

Passive reconstruction methods have additionally found use in several applications of SLAM on subsea robotics [28], where it is also possible to fuse the signals from onboard motion sensors [29]. This yields the advantage of combining MG inspection (mapping) and ROV positioning (localization), which motivates further investigation.

For both SfM and SV, many well-demonstrated implementations are available; however, the calibration of the cameras usually assumes knowledge of the refractive index between the camera lens and surrounding medium (water), which is influenced by changing environmental conditions such as pressure, temperature, and salinity, thereby complicating the application [16]. On a general note, calibration is needed in any case where the camera-based 3D reconstruction is used for precision purposes.

In summary, there are many well-demonstrated applications of passive optical reconstructions techniques, and by applying various mitigation strategies towards the physical effects inherent to the subsea environment (light attenuation, scattering etc.), these methods can and have been used with some success underwater. However, further experimental work is needed to clarify if MG provides sufficiently distinctive and detectable features.

2) Active methods: Structured Light (SL) is, in contrast to SfM and SV, an *active* method where a known pattern is projected onto the unknown scene. The intersection between the scene and pattern is reflected and used for reconstructing 3D points along the distorted pattern by triangulation. A 3D point cloud of the scene can then be created by multiple intersections obtained from changing the position of the observer or changing the pattern. Since features are actively projected onto the scene, the method is highly applicable in environments with few or no features [30]. The disadvantage in comparison to SfM/SV methods is that only spatial information is recreated, and color information valuable for MG categorization is lost. Pattern projection can be performed by a commercial light projector or a blue/green 532nm laser, where the latter is widely used in underwater applications due to the low attenuation of that specific wavelength [31]–[33]. The accuracy and range of SL methods are on par or slightly better than SfM/SV [16].

Laser Line Scanner (LLS) can be categorized into three; Continuous Wave (CW), Pulse Gated (PG), and Modulated (Mod). Continuous Wave-LSS utilizes a receiver (camera, photomultiplier tube, or photon counter) scanning back and forth along a line. A laser is pointed in a known direction along the line. The receiver detects the position of the laser point and determines the distance to the scene by triangulation. Pulse Gated-LLS uses the same general approach but synchronizes the laser source and the receiver such that the receiver opens with a delay and thereby avoids the incoming light from backscatter in the water column. Consequently, PG-LSS shows a longer working range than CW-LLS, up to 10m [34]. Modulated-LSS operates similarly to sonar by comparing a modulated source to the received reflection. The phase shift between the signals can be used to determine the distance to the object. The range and accuracy are similar to PG-LSS [16]. While the LSS only provides spatial information of a scene, Yang et al. [35] showed the feasibility of using a red/green/blue laser setup for reconstructing a small-scale underwater 3D color scene.

Time-of-Flight (ToF) utilizes the same principles as PG-LLS or Mod-LLS, but instead of scanning a single 1D line of the scene, a special ToF camera synchronized to a light source is used to capture a 3D image in one shot. Distance and grayscale information for the scene is given for each pixel. Mack et al. [36] described challenges of adapting commercial off the shelf time of flight cameras to applications underwater and demonstrated a proof-of-concept setup and initial results. UTOFIA (Underwater Time of Flight Image Acquisition) was a Horizon 2020 research project aiming to fill the gap between short-range, high-resolution conventional video and long-range low-resolution sonar systems. During the project a prototype of a range-gated ToF imaging system was developed and tested [37]. The results showed effective distance measurement at 4.5 attenuation lengths which is less than the 7 attenuation lengths obtained by PG-LSS [34]. McLeod et al. [38] published a paper covering the testing of a commercial ToF sensor. An accuracy of 1mm was obtained at a distance of 8m in a test tank, and 7mm accuracy at 30m in good visibility conditions in the ocean.

B. Acoustical methods

While light is attenuated to a much further extent in water than in air, the opposite is evident for sound. Consequently, sound has historically been extensively applied for subsea navigation and surveying over great (>1000m) distances. For the purpose of MG inspection, the distance is an order of magnitude smaller, which narrows this brief review to high frequency (>1Mhz) sonar systems. The significant advantage obtained by using sound instead of light is the independence of sonar to water turbidity. Multi-Beam Sonar (MBS) provides a thin profile image based on backscatter from objects in the trajectory of the sound beam. The range and accuracy depend on the sound frequency, where commercially available high-frequency MBS report a range of 7m and an accuracy of 0.6mm [39]. Several studies have pursued the idea to create 3D scenes from a fusion of acoustic and optical methods termed opti-acoustic imaging [40], [41]. Ferreira et al. conclude in a review of opti-acoustic imaging techniques that a general problem arises from matching acoustic and optical features [42]. During MG inspection, the size and contours of the underlying structural elements are usually known. Further work is needed to investigate if this information can be used for solving the feature matching problem in opti-acoustic imaging.

IV. Marine Growth Classification Methods

Detection and classification of marine growth from images using deep learning have been investigated in various studies with a focus ranging from the classification of species in coral reefs [43], to bio-fouling under vessels [44], [45] and finally marine fouling on offshore structures [9], [46]. As with the sensor technologies presented in the previous section, the underwater environment poses a challenge in the classification of marine growth due to the risk of poor image quality in both training images and inspection campaigns, caused by water turbidity. Furthermore, marine growth species often have indefinite shapes and ambiguous boundaries between different species leading to another challenge.

For offshore structures, the distribution of different MG species affects the loading on the structure, and various species may also affect the surface of the structure differently. Therefore the classification of the MG species, as opposed to the current spot checks, gives a better indication of the effect of the marine growth on the structure. Additionally, the ability to detect and classify MG can also lead to an estimate of the percentage cover of marine growth on structure surfaces. This knowledge will give a better basis for decision-making on cleaning campaigns. Using deep learning for the detection and classification of MG as part of the inspection of offshore structures can help automate the inspection process. However, to build a robust deep learning model, large datasets of images for training and validation are needed.

A. Datasets for training and validation

Xu et al. [47] presented a review of deep learning for marine species recognition and described a remarkable performance of deep convolutional neural networks (CNN) in visual recognition tasks, when there is a large amount of labeled data for training available. Therefore obtaining high-quality images from inspection of offshore structures is essential for achieving good results.

Chin [48] shared a dataset with a total of 1326 labeled images divided in 10 classes (algae, balanus, blue mussel, christmas tree worm, finger sponge, gooseneck barnacle, kelp, rock oysters, stinging hydrozoan and zebra mussel). Similarly, publicly available datasets exist for identification of species in coral reefs [49]. However, for the detection and classification of MG on offshore structures, larger datasets must be generated. The datasets must contain the specific MG species expected to be present at the locations of the structures to be inspected. This requires high-quality images from the current inspection sites, which can be troublesome and expensive to obtain.

Gormley et al. [9] classified MG on offshore structures using CoralNet (https://coralnet.ucsd.edu/). CoralNet, is a resource for benthic (bottom-dwelling) image analysis using deep learning, which supports fully automated annotation of images. CoralNet also works as a data repository and collaboration platform. This platform to share training data can help overcome the lack of available data. A part of the development of CoralNet is described by Beijbom et al. (2015) [50]. Using CoralNet, a number of annotation points are distributed in the images. Around each annotation point, a local image patch is extracted for classification. This helps overcome the challenge of ambiguous boundaries between MG species. An example of the ambiguous boundaries between MG species is shown in Figure 4. Gormley et al. [9] compared results of using 20 random annotation points per image, 50 points stratified random and 100 points in a uniform grid.

Fig. 4. Example of ambiguous boundaries between MG species, leading to the need for annotation points as used in CoralNet and in the work presented by Gormley et al. [9]. The image is from the port of Esbjerg.

Another way to overcome the problem of obtaining images for training deep learning models was presented by O'Byrne et al. [46], who developed a virtual scene of an underwater inspection site and trained a deep encoder-decoder network with 2500 annotated synthetic images. O'Byrne et al. [46] used two classes: soft fouling marine growth and uncolonized background. The work focused on semantic segmentation of the images, meaning that each pixel in the input image is classified. Similar to the approach with annotation points presented by Beijbom and Gormley, semantic segmentation help overcome the challenge of ambiguous boundaries between MG species. O'Byrne et al. [46] validated their proposed technique on 32 real-world underwater inspection images with 94% accuracy.

Gómez-Ríos et al. [43] aimed to enable tracking and detection of threatened and vulnerable coral species and noted that the existing publicly available databases of coral images contain *texture images* only. Texture images are defined as close-up images containing only part of the coral species. Gómez-Ríos et al. [43] wanted to develop a classifier that can classify coral species irrespective of the portion of the coral contained in each image. Therefore Gómez-Ríos et al. [43] presented a database of *structure images* containing a large part of a coral or the whole coral in each image. The texture image and structure image databases were used in a two-level classifier. The first level identifies if an image is a texture image showing only a small part of the coral or a structure image containing a large part of the coral or the whole coral. The second layer identifies the species. With the two level classifier, Gómez-Ríos et al. [43] showed that roughly 94% of test images were classified correctly.

High water turbidity may lead to a need of conducting inspection campaigns with the ROV very close to the offshore structure to get proper visual output. Oppositely, in very clear water, a larger distance to the structure may be preferred. Therefore, it should be considered to include both texture images and structure images in the training and validation datasets to make the deep learning model more robust. When a good dataset is in place, it must be decided what information is needed from the deep learning model.

B. *Classification classes*

It is important to consider which classes are necessary to obtain the most useful results of detection and classification. Different approaches to defining these classes have been used.

Chin et al. [44] defined 10 classes of different species of MG (algae, balanus, blue mussel, christmas tree worm, finger sponge, gooseneck barnacle, kelp, rock oysters, stinging hydrozoan and zebra mussel). Using transfer learning Google's Inception V3 convolutional neural network was trained to classify MG in the 10 defined classes using a dataset of 1825 labeled images. As mentioned, 1326 of these images are publicly available [48].

Xu et al. [47] noted that binary classification problems perform best. Therefore a simplification into classification of marine growth into *marine growth* and *structure surface* may lead to improved accuracy, and be sufficient to estimate the density of marine growth on the structure. Alternatively, the classes *soft marine growth*, *hard marine growth*, *structure surface*, and *background* may contain more information which is useful for determining if a cleaning campaign is needed.

Bloomfield et al. [45] used a dataset of 10263 images which were collected from underwater surveys of vessels. Instead of focusing on the marine growth species, the images were classified into three levels of growth:

- No fouling organisms, but biofilm or slime may be present
- Fouling organisms (e.g. barnacles, mussels, seaweed or tubeworms) are visible but patchy (1-15% of the surface covered)
- A large number of fouling organisms are present (16-100% of the surface covered)

Bloomfield et al. [45] used pre-trained ImageNet weights for transfer learning on different convolutional neural network architectures. These networks were used to create a network ensemble where the image class was predicted by more networks to get better performance.

If knowing the level of marine fouling is the most critical aspect of inspection campaigns, the classification classes presented by Bloomfield et al. [45] may be the most useful. However, the classes used by Chin et al. [44] do give more detailed information on the species, if that is of interest during inspection campaigns.

V. Conclusion

This paper has explored the available sensors and techniques for reducing both the operational costs and uncertainty of MG inspection results by means of automation. The two main processes showing great potential for automation are MG thickness estimation and categorization.

Several sensor technologies show potential for marine growth thickness estimation by 3D recreation of offshore structures. Low-cost optical methods such as structure from motion and stereo vision show promising results, however, main challenges such as sensitivity to low turbidity and flickering sunlight disturbances are specific issues that need further investigation for showing the usability for marine growth inspection. A possible solution for increasing robustness to low turbidity and flickering sunlight is to combine optical and acoustic sensors.

Available methods for MG classification showed to be based on deep learning relying on a large database of relevant images for training. Access to these can be difficult even though some publicly available databases exist. O'Byrne et al. proposed using virtual scenes for training to reduce the need for real images. Classification categories vary from detailed classification into several MG species to classification of the level of marine growth. The level of detail needed to determine if a cleaning campaign is required must be considered when choosing classification classes for inspection of offshore structures.

Acknowledgements

The authors would like to thank for the support from the Energy Technology Development and Demonstration Programme (EUDP) via the "ACOMAR – Auto Compact Marine Growth Remover" project (J.No. 64020-1093). Thanks also go to our project partners SubC Partner, Sihm Højtryk, Mati2ilt, Total E&P Denmark and Siemens Gamesa Renewable Energy, and our colleagues from Aalborg University, for many valuable discussions and technical support.

References

[1] T. Yan and W. X. Yan, "Fouling of Offshore Structures in China-a Review," *Biofouling*, vol. 19, no. sup1, pp. 133–138, 1 2003.

[2] R. Miller and A. Macleod, "Marine Growth Mapping and Monitoring: Feasibility of Predictive Mapping of Marine Growth March. A report by SAMS Research Services Ltd to the Offshore Renewable Energy Catapult." no. March, p. 69, 2016.

[3] A. Theophanatos and J. Wolfram, "Hydrodynamic Loading on Macro-Roughened Cylinders of Various Aspect Ratios," *Journal of Offshore Mechanics and Arctic Engineering*, vol. 111, no. 3, pp. 214–222, 1989. [Online]. Available: https://doi.org/10.1115/1.3257150

[4] Det Norske Veritas, *Design of Offshore Wind Turbines Structures DNV-OS-J101*, 2013.

[5] W. Shi, H. C. Park, J. H. Baek, C. W. Kim, Y. C. Kim, and H. K. Shin, "Study on the marine growth effect on the dynamic response of offshore wind turbines," *International Journal of Precision Engineering and Manufacturing*, vol. 13, no. 7, pp. 1167–1176, 2012.

[6] J. P. Lord, "Impact of seawater temperature on growth and recruitment of invasive fouling species at the global scale," *Marine Ecology*, vol. 38, no. 2, p. e12404, 2017. [Online]. Available: https://onlinelibrary.wiley.com/doi/abs/10.1111/maec.12404

[7] C. Wright, J. Murphy, and V. Pakrashi, "The dynamic effects of marine growth on a tension moored floating wind turbine," *Progress in Renewable Energies Offshore - Proceedings of 2nd International Conference on Renewable Energies Offshore, RENEW 2016*, no. October, pp. 723–732, 2016.

[8] C. Wright, J. Murphy, C. S. W. V. Pakrashi, and J. Murphy, "The Dynamic Effects of Marine Growth on a Point Absorbing Wave Energy," *In Proceedings of the Offshore Energy & Storage Symposium and Industry Connector*, no. July, pp. 1–5, 2016.

[9] K. Gormley, F. McLellan, C. McCabe, C. Hinton, J. Ferris, D. I. Kline, and B. E. Scott, "Automated image analysis of offshore infrastructure marine biofouling," *Journal of Marine Science and Engineering*, vol. 6, no. 1, pp. 1–20, 2018.

[10] S. Pedersen, J. Liniger, F. F. Sorensen, and M. von Benzon, "On Marine Growth Removal on Offshore Structures," in *Proceedings of the IEEE OCEANS 2022 conference*, Chennai, 2 2022, pp. 1–5.

[11] Energinet, "Technical Project Description for Offshore Wind Farms (200 MW) Report nr. 13-97289-2," Energinet.dk, DK-7000 Fredericia, Tech. Rep., 4 2015. [Online]. Available: www.ens.dk

[12] Z. Wang, R. Hu, H. Leng, H. Liu, Y. Bai, and W. Lu, "Deformation Analysis of Large Diameter Monopiles of Offshore Wind Turbines under Scour," *Applied Sciences*, vol. 10, no. 21, p. 7579, 10 2020.

[13] M. Borg, M. W. Jensen, S. Urquhart, M. T. Andersen, J. B. Thomsen, and H. Stiesdal, "Technical definition of the tetraspar demonstrator floating wind turbine foundation," *Energies*, vol. 13, no. 18, 9 2020.

[14] B. Chemisky, F. Menna, E. Nocerino, and P. Drap, "Underwater survey for oil and gas industry: A review of close range optical methods," *Remote Sensing*, vol. 13, no. 14, pp. 1–31, 2021.

[15] F. Menna, P. Agrafiotis, and A. Georgopoulos, "State of the art and applications in archaeological underwater 3D recording and mapping," *Journal of Cultural Heritage*, vol. 33, pp. 231–248, 2018. [Online]. Available: http://dx.doi.org/10.1016/j.culher.2018.02.017

[16] M. Massot-Campos and G. Oliver-Codina, "Optical sensors and methods for underwater 3D reconstruction," *Sensors (Switzerland)*, vol. 15, no. 12, pp. 31 525–31 557, 12 2015.

[17] Q. Xi, T. Rauschenbach, and L. Daoliang, "Review of underwater machine vision technology and its applications," *Marine Technology Society Journal*, vol. 51, no. 1, pp. 75–97, 2017.

[18] F. Santoso, M. A. Garratt, M. R. Pickering, and M. Asikuzzaman, "3D Mapping for Visualization of Rigid Structures: A Review and Comparative Study," *IEEE Sensors Journal*, vol. 16, no. 6, pp. 1484–1507, 2016.

[19] J. Jaffe, "Underwater optical imaging: status and prospects," *Oceanography : the official magazine of the Oceanography Society.*, vol. 14, no. 3, p. 66, 2001.

[20] S. Q. Duntley, "Light in the Sea*," *Journal of the Optical Society of America*, vol. 53, no. 2, pp. 214–233, 2 1963.

[21] M. Ludvigsen, R. Eustice, and H. Singh, "Photogrammetric models for marine archaeology," Tech. Rep.

[22] T. Nicosevici, N. Gracias, S. Negahdaripour, and R. Garcia, "Efficient three-dimensional scene modeling and mosaicing," *Journal of Field Robotics*, vol. 26, no. 10, pp. 759–788, 10 2009.

[23] F. Bruno, A. Gallo, F. De Filippo, M. Muzzupappa, B. Davidde Petriaggi, and P. Caputo, "3D documentation and monitoring of the experimental cleaning operations in the underwater archaeological site of Baia (Italy)," in *2013 Digital Heritage International Congress (DigitalHeritage)*. IEEE, 10 2013, pp. 105–112.

[24] D. McKinnon, H. He, B. Upcroft, and R. N. Smith, "Towards automated and in-situ, near-real time 3-D reconstruction of coral reef environments," *OCEANS'11 - MTS/IEEE Kona, Program Book*, 2011.

[25] M. Bryson, M. Johnson-Roberson, O. Pizarro, and S. Williams, "Colour-Consistent Structure-from-Motion Models using Underwater Imagery," in *Robotics: Science and Systems VIII*. Robotics: Science and Systems Foundation, 7 2012.

[26] B. Liu, Z. Liu, S. Men, Y. Li, Z. Ding, J. He, and Z. Zhao, "Underwater Hyperspectral Imaging Technology and Its Applications for Detecting and Mapping the Seafloor: A Review," *Sensors*, vol. 20, no. 17, p. 4962, 9 2020. [Online]. Available: https://www.mdpi.com/1424-8220/20/17/4962

[27] M. Reggiannini and D. Moroni, "The use of saliency in underwater computer vision: A review," *Remote Sensing*, vol. 13, no. 1, pp. 1–26, 2021.

[28] Y. Wu, X. Ta, R. Xiao, Y. Wei, D. An, and D. Li, "Survey of underwater robot positioning navigation," *Applied Ocean Research*, vol. 90, p. 101845, 2019. [Online]. Available: http://www.sciencedirect.com/science/article/pii/S0141118718305546

[29] I. Mahon, S. Williams, O. Pizarro, and M. Johnson-Roberson, "Efficient View-Based SLAM Using Visual Loop Closures," *IEEE Transactions on Robotics*, vol. 24, no. 5, pp. 1002–1014, 10 2008.

[30] S. Narasimhan and S. Nayar, "Structured Light Methods for Underwater Imaging: Light Stripe Scanning and Photometric Stereo," in *Proceedings of OCEANS 2005 MTS/IEEE*. IEEE, pp. 1–8.

[31] T. Nakatani, S. Li, T. Ura, A. Bodenmann, and T. Sakamaki, "3D visual modeling of hydrothermal chimneys using a rotary laser scanning system," in *2011 IEEE Symposium on Underwater Technology and Workshop on Scientific Use of Submarine Cables and Related Technologies*. IEEE, 4 2011, pp. 1–5.

[32] M. Prats, J. J. Fernandez, and P. J. Sanz, "An approach for semi-autonomous recovery of unknown objects in underwater environments," in *2012 13th International Conference on Optimization of Electrical and Electronic Equipment (OPTIM)*. IEEE, 5 2012, pp. 1452–1457.

[33] M. Massot-Campos, G. Oliver-Codina, H. Kemal, Y. Petillot, and F. Bonin-Font, "Structured light and stereo vision for underwater 3D reconstruction," in *OCEANS 2015 - Genova*. IEEE, 5 2015, pp. 1–6.

[34] F. R. Dalgleish, F. M. Caimi, W. B. Britton, and C. F. Andren, "Improved LLS imaging performance in scattering-dominant waters," W. W. Hou, Ed., 5 2009, p. 73170E.

[35] Y. Yang, B. Zheng, L.-Y. Kan, J. Yu, and J.-C. Wang, "3D color reconstruction based on underwater RGB laser line scanning system," *Optik*, vol. 125, no. 20, pp. 6074–6077, 10 2014.

[36] K. V. Mack, W. D. Jemison, L. K. Rumbaugh, D. W. Illig, and M. K. Banavar, "Time-of-flight (ToF) cameras for underwater situational awareness," in *OCEANS 2019 MTS/IEEE Seattle, OCEANS 2019*, 2019, pp. 12–16.

[37] P. Risholm, J. Thorstensen, J. T. Thielemann, K. Kaspersen, J. Tschudi, C. Yates, C. Softley, I. Abrosimov, J. Alexander, and K. H. Haugholt, "Real-time super-resolved 3D in turbid water using a fast range-gated CMOS camera," *Applied Optics*, vol. 57, no. 14, p. 3927, 5 2018.

[38] D. McLeod, J. Jacobson, M. Hardy, and C. Embry, "Autonomous inspection using an underwater 3D LiDAR system," *2013 OCEANS - San Diego*, pp. 1–8, 2013.

[39] Teledyne Marine, "BlueView M900-2250-S 130/45," 12 2021. [Online]. Available: http://www.teledynemarine.com/M900-2250-S_130-45-Mk2

[40] N. Hurtos, X. Cufi, and J. Salvi, "Calibration of optical camera coupled to acoustic multibeam for underwater 3D scene reconstruction," in *OCEANS'10 IEEE SYDNEY*. IEEE, 5 2010, pp. 1–7.

[41] S. Negahdaripour, H. Sekkati, and H. Pirsiavash, "Opti-Acoustic Stereo Imaging: On System Calibration and 3-D Target Reconstruction," *IEEE Transactions on Image Processing*, vol. 18, no. 6, pp. 1203–1214, 6 2009.

[42] F. Ferreira, D. Machado, G. Ferri, S. Dugelay, and J. Potter, "Underwater optical and acoustic imaging: A time for fusion? a brief overview of the state-of-the-art," in *OCEANS 2016 MTS/IEEE Monterey, OCE 2016*. Institute of Electrical and Electronics Engineers Inc., 11 2016.

[43] A. Gómez-Ríos, S. Tabik, J. Luengo, A. Shihavuddin, and F. Herrera, "Coral species identification with texture or structure images using a two-level classifier based on Convolutional Neural Networks," *Knowledge-Based Systems*, vol. 184, p. 104891, 11 2019. [Online]. Available: https://linkinghub.elsevier.com/retrieve/pii/S0950705119303569

[44] C. S. Chin, J. T. Si, A. S. Clare, and M. Ma, "Intelligent Image Recognition System for Marine Fouling Using Softmax Transfer Learning and Deep Convolutional Neural Networks," *Complexity*, vol. 2017, 2017.

[45] N. J. Bloomfield, S. Wei, B. A. Woodham, P. Wilkinson, and A. P. Robinson, "Automating the assessment of biofouling in images using expert agreement as a gold standard," *Scientific Reports*, vol. 11, no. 1, p. 2739, 12 2021. [Online]. Available: http://www.nature.com/articles/s41598-021-81011-2

[46] M. O'Byrne, V. Pakrashi, F. Schoefs, and B. Ghosh, "Semantic segmentation of underwater imagery using deep networks trained on synthetic imagery," *Journal of Marine Science and Engineering*, vol. 6, no. 3, 2018.

[47] L. Xu, M. Bennamoun, S. An, F. Sohel, and F. Boussaid, "Deep Learning for Marine Species Recognition," 2019, pp. 129–145. [Online]. Available: http://link.springer.com/10.1007/978-3-030-11479-4_7

[48] C. Chin, "Marine Fouling Images," *IEEE Dataport*, 2019. [Online]. Available: https://ieee-dataport.org/documents/marine-fouling-images

[49] A. SHIHAVUDDIN, "Coral reef dataset," *Mendeley Data*, vol. V2, 2017.

[50] O. Beijbom, P. J. Edmunds, C. Roelfsema, J. Smith, D. I. Kline, B. P. Neal, M. J. Dunlap, V. Moriarty, T.-Y. Fan, C.-J. Tan, S. Chan, T. Treibitz, A. Gamst, B. G. Mitchell, and D. Kriegman, "Towards Automated Annotation of Benthic Survey Images: Variability of Human Experts and Operational Modes of Automation," *PLOS ONE*, vol. 10, no. 7, 7 2015.